BIOLOGY OF REPRODUCTION **53,** 985–995 (1995)

Effect of Cryoprotectant Solutes on Water Permeability of Human Spermatozoa[1]

J.A. Gilmore,[3,4] L.E. McGann,[5] J. Liu,[3,6] D.Y. Gao,[3] A.T. Peter,[4] F.W. Kleinhans,[3,6] and J.K. Critser[2,3,4,7]

Cryobiology Research Institute,[3] Methodist Hospital of Indiana, Indianapolis, Indiana
Department of Veterinary Clinical Sciences,[4] School of Veterinary Medicine
Purdue University, West Lafayette, Indiana
Department of Laboratory Medicine and Pathology,[5] University of Alberta, Edmonton, Alberta, Canada
Department of Physics,[6] Indiana University-Purdue University at Indianapolis, Indianapolis, Indiana
Departments of Physiology/Biophysics and Obstetrics/Gynecology[7]
Indiana University School of Medicine, Indianapolis, Indiana

ABSTRACT

Osmotic permeability characteristics and the effects of cryoprotectants are important determinants of recovery and function of spermatozoa after cryopreservation. The primary purpose of this study was to determine the osmotic permeability parameters of human spermatozoa in the presence of cryoprotectants. A series of experiments was done to: 1) validate the use of an electronic particle counter for determining both static and kinetic changes in sperm cell volume; 2) determine the permeability of the cells to various cryoprotectants; and 3) test the hypothesis that human sperm water permeability is affected by the presence of cryoprotectant solutes. The isosmotic volume of human sperm was 28.2 ± 0.2 μm^3 (mean ± SEM), 29.0 ± 0.3 μm^3, and 28.2 ± 0.4 μm^3 at 22, 11, and 0°C, respectively, measured at 285 mOsm/kg via an electronic particle counter. The osmotically inactive fraction of human sperm was determined from Boyle van't Hoff (BVH) plots of samples exposed to four different osmolalities (900, 600, 285, and 145 mOsm/kg). Over this range, cells behaved as linear osmometers with osmotically inactive cell percentages at 22, 11, and 0°C of 50 ± 1%, 41 ± 2%, and 52 ± 3%, respectively. Permeability of human sperm to water was determined from the kinetics of volume change in a hyposmotic solution (145 mOsm/kg) at the three experimental temperatures. The hydraulic conductivity (L_p) was 1.84 ± 0.06 $\mu m \cdot min^{-1} \cdot atm^{-1}$, 1.45 ± 0.04 $\mu m \cdot min^{-1} \cdot atm^{-1}$, and 1.14 ± 0.07 $\mu m \cdot min^{-1} \cdot atm^{-1}$ at 22, 11, and 0°C, respectively, yielding an Arrhenius activation energy (E_a) of 3.48 kcal/mol. These biophysical characteristics of human spermatozoa are consistent with findings in previous reports, validating the use of an electronic particle counter for determining osmotic permeability parameters of human sperm. This validated system was then used to investigate the permeability of human sperm to four different cryoprotectant solutes, i.e., glycerol (Gly), dimethylsulfoxide (DMSO), propylene glycol (PG), and ethylene glycol (EG), and their effects on water permeability. A preloaded, osmotically equilibrated cell suspension was returned to an isosmotic medium while cell volume was measured over time. A Kedem-Katchalsky model was used to determine the permeability of the cells to each solute and the resulting water permeability. The permeabilities of human sperm at 22°C to Gly, DMSO, PG, and EG were 2.07 ± 0.13 × 10^{-3} cm/min, 0.80 ± 0.02 × 10^{-3} cm/min, 2.3 ± 0.1 × 10^{-3} cm/min, and 7.94 ± 0.67 × 10^{-3} cm/min, respectively. The resulting L_p values at 22°C were reduced to 0.77 ± 0.08 $\mu m \cdot min^{-1} \cdot atm^{-1}$, 0.84 ± 0.07 $\mu m \cdot min^{-1} \cdot atm^{-1}$, 1.23 ± 0.09 $\mu m \cdot min^{-1} \cdot atm^{-1}$, and 0.74 ± 0.06 $\mu m \cdot min^{-1} \cdot atm^{-1}$, respectively. These data support the hypothesis that low-molecular-weight, nonionic cryoprotectant solutes affect (decrease) human sperm water permeability.

INTRODUCTION

The cryopreservation of human spermatozoa has become a requirement in artificial insemination programs. The primary reason is that cryopreservation allows time between the collection of the sample and insemination to screen for sexually transmitted diseases in the donors, including the human immunosuppressive virus (HIV) that results in the life-threatening illness Acquired Immune Deficiency Syndrome (AIDS) [1]. In addition, cryopreservation of semen serves as a means of preserving reproductive potential for males who undergo various types of chemotherapy, radiation, or surgical techniques that may ultimately result in iatrogenic sterility.

In order to optimally cryopreserve spermatozoa, it is crucial to understand certain physical and biophysical characteristics of these cells. There are five primary properties with particular significance to cryopreservation: 1) the hydraulic conductivity (L_p), which reflects the membrane's permeability to water; 2) the osmotically inactive fraction of cell volume (V_b); 3) the isosmotic cell volume (V_{iso}), which is the volume of the cell existing in osmotic equilibrium with an isosmotic solution; 4) the activation energy for L_p (E_a), which is the temperature dependence of L_p; and 5) the permeability coefficient for the cryoprotectant solute (P_{CPA}).

During cryopreservation, if the cooling rate is relatively too rapid, intracellular water will not be removed quickly enough, resulting in intracellular ice formation that is generally lethal. If the rate is relatively too slow, the cells are exposed to the high solute concentration outside the cell for an excessive time interval and are damaged by solute

Accepted June 5, 1995.
Received March 13, 1995.
[1]This work was supported by Methodist Hospital of Indiana, Inc., a Career Development Award from the NIH (KO4-HD00980 to J.K.C.), a grant from the USDA/NRICGP (93-37203-9272 to J.K.C. and A.T.P.) and a NATO Collaborative Research Grant (CRG 920170 to J.K.C.).
[2]Correspondence: John K. Critser, Ph.D., Cryobiology Research Institute, Methodist Hospital of Indiana, 1701 N. Senate Blvd.—Wile Hall Room 611, Indianapolis, IN 46206-1367. FAX: (317) 929-5347.

effects [2]. The E_a for L_p, in conjunction with the water permeability coefficient, allows calculation of the maximum rate at which human spermatozoa can be cooled while intracellular freezing is avoided [2]. This information is crucial for optimizing cryopreservation protocols and minimizing cellular damage. The hydraulic conductivity for human spermatozoa has been previously measured through use of a "time-to-lysis" technique [3], an approach utilizing the critical osmolality of human sperm at which 50% of the cells swell and lyse, which is achieved after a cell has swelled to its maximum tolerated volume.

Cryoprotectant agents (CPAs) are required for the cryopreservation of most cell types, such as red blood cells (RBC), lymphocytes, hematopoietic stem cells, spermatozoa, and embryos. While glycerol (Gly) is the most commonly used CPA for cryopreservation of human spermatozoa, dimethylsulfoxide (DMSO), ethylene glycol (EG; 1,2-ethanediol), and propylene glycol (PG; 1,2-propanediol) are cryoprotectants used commonly with other cells and tissues. In general, because CPAs are maximally effective after equilibration across the plasma membrane, it is important to determine the permeability coefficients of the cells to cryoprotectants (P_{CPA}) and their associated effect on osmotically driven cell volume excursions [4]. It is equally important to determine the effect of the CPAs on cell properties such as hydraulic conductivity.

Previous studies have determined the permeability of human sperm to glycerol (P_{gly}) using a "time-to-lysis" technique [5] and an electron paramagnetic resonance technique [6]. Some effects of DMSO have also been studied for human sperm [7]. However, little is known about the permeability of spermatozoa to CPAs other than Gly. High reported values for L_p [3] imply that human sperm theoretically should be able to survive extremely rapid cooling rates [3], a prediction that was not supported by experimental observation when cells were cooled at 800°C/min [8]. One possible explanation for this discrepancy between theory and observation is that the presence of a CPA changes the sperm plasma membrane's water permeability, a hypothesis tested in this study.

Electronic particle counters have previously been used to determine cell membrane permeability characteristics. Granulocytes (leukocytic blood cells) and cytoplasts (membrane-bound units of cytoplasm) are two representative cases for which an electronic particle counter was used to measure the change in cell volume as a function of time [9]. A number of plant cells have also been studied to determine change in size via an electronic particle counter [10].

The objectives of this study were to 1) validate the use of an electronic particle counter for determining both static and kinetic changes in sperm cell volume; 2) determine the permeability of the cells to various cryoprotectants; and 3) test the hypothesis that human sperm water permeability is affected by the presence of cryoprotectant solutes.

MATERIALS AND METHODS

Samples

Semen samples were obtained, with informed consent, from healthy donors by masturbation. The samples were obtained after at least 48 hours of sexual abstinence. A minimum concentration of 2×10^7 spermatozoa per milliliter, with at least 40% motility, was required for the samples to be included in the study. The ejaculates were allowed to liquefy in an incubator (5% CO_2:95% air, 37°C, and high humidity) for 30 min. Samples were layered on a discontinuous (90% and 47%) Percoll gradient to select for motile cells and then washed with a Tyrode's lactate Hepes (TL Hepes)-buffered solution (285 mOsm/kg) [11] supplemented with pyruvate (0.01 mg/ml) and resuspended to approximately 2.5 ml final sample volume. A fraction of the sample (5 μl) was analyzed using computer-assisted semen analysis (CASA) (Cell Soft, Version 3.2/C; CRYOResources, LTD., Montgomery, NY). Subsequent CASA analysis was done at the completion of each experiment.

Media

The media used were derivatives of an isosmotic TL Hepes solution (285 mOsm/kg). The media were diluted with distilled water to make a hyposmotic solution: 0.5 × TL Hepes (145 mOsm/kg). Two hyperosmotic solutions were made by diluting 1 M sucrose with isosmotic TL Hepes medium: 1) 0.3 M sucrose (600 mOsm/kg net) and 2) 0.5 M sucrose (900 mOsm/kg net). Osmolality was determined via a freezing-point depression osmometer (Model 3D2; Advanced Instruments, Needham Heights, MA), and osmolalities are accurate to ± 5 mOsm/kg. The cryoprotectant treatment solutions were prepared by mixing Gly, DMSO, PG, or EG with TL Hepes to yield CPA concentrations of 2 M (Gly, DMSO, and PG) and 4 M (EG). All media used in the experiments were obtained from Sigma Chemical Company (St. Louis, MO).

Flow Cytometry

Sperm viability was measured using a dual fluorescent staining technique [3, 5, 12] in conjunction with the FACStar Plus Analyzer (Becton Dickinson, Rutherford, NJ). Stock solutions of carboxyfluorescein diacetate (CFDA) and propidium iodide (PI) were prepared by mixing 2.5 mg CFDA/ml with DMSO and 0.5 mg PI/ml with water. Cells were exposed to 10 μl/ml of CFDA and 10 μl/ml of PI at a minimum cell concentration of 2×10^7 cells/ml. CFDA permeates membrane-intact cells and fluoresces green, whereas PI enters membrane-damaged cells and fluoresces red. Samples containing the cells and the two fluorescent stains were mixed thoroughly at room temperature and analyzed in the flow cytometer within 10–30 min of exposure to the stains. The cells that stained CFDA-positive and PI-negative

TABLE 1. Definitions of major symbols used in equations.

Symbol	Description	Units	Value
L_p	water permeability	$\mu m \cdot min^{-1} \cdot atm^{-1}$	parameter
P_{CPA}	CPA permeability	cm/min	parameter
A_c	surface area of human spermatozoa	μm^2	120
V_b	osmotically inactive cell volume	μm^3	50%
V_a	volume of osmotically inactive water	μm^3	9%
V_s	total cell solids	μm^3	41%
V_w	total cell water	μm^3	59%
V	total cell volume	μm^3	28.2
M	osmolality	osm/kg H_2O	—
σ	reflection coefficient	—	parameter
N	moles of solute inside cell	moles	variable
C	concentrations	molal	variable
iso	subcripts (iso = isosmolality,	—	—
salt	salt = impermeable salts,		
CPA	CPA = cryoprotectant)		
e,i	superscripts (e = external, i = internal)	—	—
$\bar{V}$	partial molar volume	L/mol	variable

were considered membrane intact. Those cells that were dual stained (< 10%) were excluded from the experiment due to questionable membrane integrity.

Electronic Particle Counter

A Coulter counter (ZM model; Coulter Electronics, Inc., Hialeah, FL) with a standard 50-μm aperture tube was used for all measurements. Volumes (V) were calibrated in each experimental solution via spherical styrene beads (Duke Scientific Corporation, Palo Alto, CA) with a diameter of 3.98 ± 0.03 μm (V = 33.1 μm^3). The relationship between conductivity and styrene bead volume was assumed to be the same as the relationship between conductivity and sperm volume.

Data Acquisition

The Coulter counter was interfaced to a microcomputer using a CSA-1S interface (The Great Canadian Computer Company, Alberta, CA). Two data acquisition modes are supported. The first produces a histogram (volume distribution) of particle count vs. volume, V(n). In the second mode, the average cell volume vs. time, V(t), is generated by computing the average cell volume over short (220 msec) time intervals, typically using 500 cells per determination.

Data Analysis

The mean, standard error, and coefficient of variation were computed within and among donors, and data were examined by standard analysis of variance approaches with the Statistical Analysis Software (SAS) program, a software system for data analysis (SAS Institute Inc., Cary, NC).

Cell osmotic response. It was hypothesized that human sperm behave as linear osmometers. This means that the cell equilibrium volume is a linear function of the reciprocal of the extracellular osmolality of solutes (assuming the cell membrane is impermeable to all solutes), which is described by the following equation (Boyle van't Hoff [BVH] relationship):

$$\frac{V}{V_{iso}} = \frac{M_{iso}}{M}\left(1 - \frac{V_b}{V_{iso}}\right) + \frac{V_b}{V_{iso}} \quad [1]$$

where V is the cell volume at the osmolality *M*, V_{iso} is the cell volume at isosmolality (M_{iso}), and V_b is the osmotically inactive cell volume (including both cell solids and osmotically inactive water). The linear osmometer hypothesis was examined in the present study by plotting experimentally measured, normalized cell equilibrium volume (V/V_{iso}) vs. the reciprocal of normalized osmolality (M_{iso}/M). Numerical values of all constants and appropriate units are shown in Table 1.

Membrane transport parameters. The Kedem-Katchalsky membrane transport model [13] was used to theoretically characterize the cell volume change in response to anisosmotic conditions. The mathematical formulation includes two coupled first-order nonlinear ordinary differential equations that describe the total transmembrane volume flux and the transmembrane permeable solute flux, respectively. For the case of a solution consisting of a single permeable solute (e.g., Gly) and other impermeable solutes (salts), the equations are:

$$J_v = \frac{1}{A_c}\frac{dV(t)}{dt} = -L_p\{(C^e_{salt} - C^i_{salt}) + \sigma(C^e_{CPA} - C^i_{CPA})\}RT \quad [2]$$

$$J_{CPA} = \frac{1}{A_c}\frac{dN_{CPA}}{dt} = \bar{C}_{CPA}(1 - \sigma)J_v + P_{CPA}(C^e_{CPA} - C^i_{CPA}) \quad [3]$$

where J_v = total volume flux, V = sperm volume, t = time, N_{CPA} = moles of permeable solute inside the cell, A_c = sperm surface area (120 μm^2) [6], L_p = water permeability

coefficient of the human sperm membrane, C = molal concentration of solute, J_{CPA} = CPA flux across the cell membrane, superscript e = extracellular, superscript i = intracellular, σ = reflection coefficient of cell membrane to the CPA, P_{CPA} = CPA permeability coefficient of cell membrane, $\bar{C}_{CPA}$ = average of extracellular and intracellular CPA concentrations, $\bar{C}_{CPA} = (C^e_{CPA} - C^i_{CPA})/[\ln(C^e_{CPA}/C^i_{CPA})]$, R = universal gas constant, and T = absolute temperature.

Intracellular concentrations of impermeable solute and permeable solute (CPA) can be calculated as:

$$C^i_{salt}(t) = C^i_{salt}(0)\left(\frac{V(0) - V_b - \bar{V}_{CPA}N^i_{CPA}(0)}{V(t) - V_b - \bar{V}_{CPA}N^i_{CPA}(t)}\right) \quad [4]$$

$$C^i_{CPA}(t) = \left(\frac{N^i_{CPA}(t)}{V(t) - V_b - \bar{V}_{CPA}N^i_{CPA}(t)}\right) \quad [5]$$

where V_b = osmotically inactive cell volume, $\bar{V}_{CPA}$ = partial molar volume of CPA, N = moles of CPA inside the cell, and 0 = initial condition (t = 0). Initial conditions for V(0), $C^i_{salt}(0)$, $C^i_{CPA}(0)$, $N^i_{CPA}(0)$ were known on the basis of each experimental protocol. In computer simulations, it was assumed a) that extracellular concentrations of permeating (C^e_{CPA}) and nonpermeating solutes (C^e_{salt}) were constant, and b) that the mixing of solutions during the CPA addition and removal was instantaneous.

Equations [4] and [5] require the partial molar volumes of the cryoprotectants, $\bar{V}P_{CPA}$. These were computed from solution tables in the *Handbook of Chemistry and Physics* [14] for Gly, EG, and PG, yielding values of $\bar{V}_{Gly}$ = 71 ml/mol, $\bar{V}_{EG}$ = 54 ml/mol, and $\bar{V}_{PG}$ = 70 ml/mol. For DMSO, $\bar{V}_{DMSO}$ = 69 ml/mol [15].

In the absence of cryoprotectant, these transport equations reduce to a single equation describing the water flux across the cell membrane [16]:

$$\frac{dV(t)}{dt} = -L_pA_c(C^e_{salt} - C^i_{salt})RT. \quad [6]$$

Membrane transport parameter fits to the kinetic volume data were performed using the software package SLAB (Civilized Software 1993, Bethesda, MD), which solves differential equations using the Gear method [17] and iterates the solution to find the best fit parameters using the Marquardt-Levenberg method [17].

The water and solute permeabilities are readily fit with this methodology. However, the signal-to-noise ratio of the data was not high enough to allow a determination of σ. For the reasons outlined in *Discussion*, the decision was made to assume that there is no interaction between the water and solute flux in this system. This reduces the system to a two-parameter (L_p and P_{CPA}) transport model where σ is no longer an independent parameter but is given by $\sigma = 1 - (P_{CPA}\bar{V}_{CPA})/(RTL_p)$ [13].

Activation energy. The activation energy (E_a) of the hydraulic conductivity (L_p) was calculated from the following Arrhenius relationship, which is assumed to describe the temperature dependence of cell membrane permeabilities [18]:

$$L_p(T) = L_p(T_o)\exp\left[-\frac{E_a}{R}\left(\frac{1}{T} - \frac{1}{T_o}\right)\right] \quad [7]$$

where L_p is the hydraulic conductivity of the cell membrane at temperature T(K), and $L_p(T_0)$ is the hydraulic conductivity at a reference temperature T_0.

Experimental Design

Experiment 1: Determination of human sperm cell isosmotic volume. This experiment was designed to determine isosmotic human sperm cell volume at three experimental temperatures. After the cell sample was processed, 100 µl of cell suspension was diluted into 10 ml of isosmotic (285 mOsm/kg) TL Hepes solution. Mean cell volumes were measured 3 min after exposure of the cell suspension to experimental solutions of 145 to 900 mOsm/kg in triplicate experimental runs at each of the experimental temperatures (22, 11, and 0°C). Experimental temperatures were measured through use of a thermocouple directly before and after each 30-sec experimental run and kept within ± 2°C (room temperature at 22°C, a cooling bath at 11°C, and an ice-water bath at 0°C). At each temperature, the experimental solutions, the cell sample, the aperture tube, the calibration beads, and the pipette tips were preequilibrated to the experimental temperature. Samples from a total of five donors (n = 5) were used at each experimental temperature.

Experiment 2: Cell osmotic response and inactive volume (V_b). This experiment was designed to verify that human sperm cells respond as linear osmometers and to determine the osmotically inactive fraction of cell volume. Kinetic volume analysis was used to confirm that the cells were in osmotic equilibrium in the anisosmotic solutions before equilibrium volumes were determined from histograms of volume distribution. A total of five donors (n = 5) was used.

Experiment 3: Determination of L_p and E_a in the absence of CPA. This experiment was designed to determine the hydraulic conductivity of sperm cells at 22, 11, and 0°C and the activation energy (E_a). Experimental temperatures were maintained within ± 2°C during each run (room temperature at 22°C, a cooling bath at 11°C, and an ice-water bath at 0°C). The cells suspension and all necessary equipment (media, aperture, pipette tips, and Coulter vials) were preequilibrated to the desired experimental temperature; then 100 µl of the sample was abruptly diluted into 10 ml of the hyposmotic solution (145 mOsm/kg), and the resulting kinetic data were recorded. Isosmotic cell volumes were measured prior to each experiment. A total of five donors (n = 5) were used at each experimental temperature.

TABLE 2. The isosmotic cell volume of human sperm at different temperatures.

Temperature[a] (°C)	Volume (μm^3)	Sample size (n)	CV[b] within donors (%)	CV among donors (%)
22	28.2 ± 0.2[c]	5	2.9	1.8
11	29.0 ± 0.3	5	9.2	2.4
0	28.2 ± 0.5	5	7.5	3.5
Mean ± SEM across temperatures	28.5 ± 0.3			

[a]There was no significant difference across temperatures ($p = 0.11$).
[b]Coefficient of variation.
[c]Mean ± SEM.

Experiment 4: Determination of L_p^{CPA} and P_{CPA} for Gly, DMSO, PG, and EG. This experiment was designed to determine the permeability of the cells to Gly, DMSO, PG, and EG at 22°C and the corresponding hydraulic conductivity in the presence of CPA (L_p^{CPA}). The experimental conditions were chosen to maximize the magnitude and duration of the cell volume excursion without damaging the cells [19]. One hundred microliters of 2 M Gly, DMSO, or PG was added drop by drop over 60 sec to 100 µl of cell suspension at 22°C, giving a final concentration of 1 M CPA. Because of the high P_{EG} found, it was necessary to double the EG concentration in order to obtain a measurable cell response.

Cells were allowed to equilibrate in the CPA solution for approximately 3 min; then 200 µl of cell suspension was abruptly diluted into isosmotic media (285 mOsm/kg) and the kinetic data recorded. A total of five donors (n = 5) was used with each CPA.

RESULTS

Experiment 1: Determination of Human Sperm Isosmotic Volume

Human sperm isosmotic volumes were determined at 22, 11, and 0°C (Table 2). The cell volume was independent of temperature ($p = 0.11$), yielding an average cell volume of 28.5 μm^3; however, there was a significant main effect of donor on volume at 22 and 11°C ($p = 0.01$). The variability among donors was relatively small, with a coefficient of variation (CV) ≤ 3.5%.

Experiment 2: Cell Osmotic Response and Inactive Volume (V_b)

Figure 1 illustrates typical volume histograms of cells exposed to isosmotic and hyposmotic solutions, showing that the population is osmotically active.

The osmotic volume response of the cells over the range 145–900 mOsm/kg is presented as BVH plots (Fig. 2); a linear osmotic response is shown at the three experimental temperatures. The osmotically inactive cell volume (V_b)

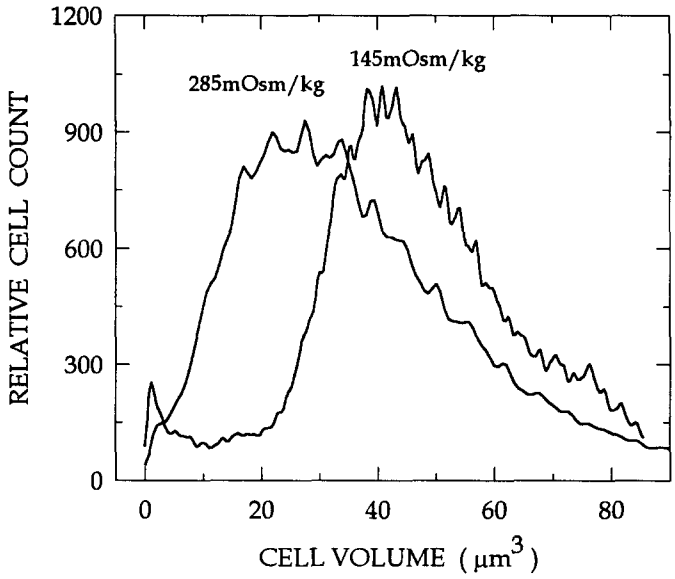

FIG. 1. Volume distributions of human sperm. The sperm sample was exposed to 1) isosmotic TL Hepes (285 mOsm/kg) and 2) hyposmotic TL Hepes (145 mOsm/kg) for 3 min before analysis.

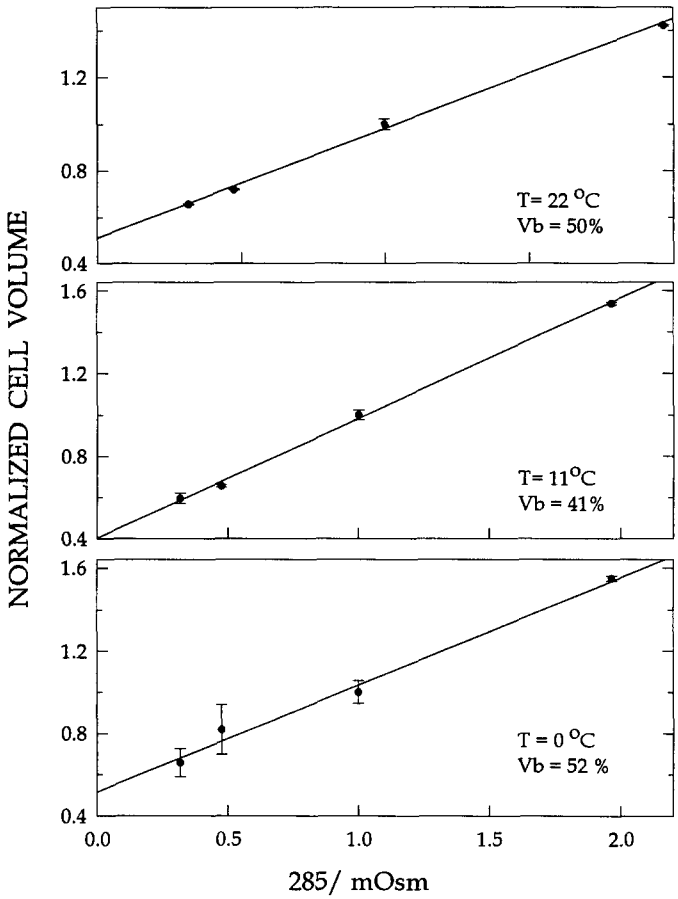

FIG. 2. BVH plots of human sperm at 22, 11, and 0°C. The sperm samples were exposed to four different osmolalities: 1) 900 mOsm/kg, 2) 600 mOsm/kg, 3) 285 mOsm/kg, and 4) 145 mOsm/kg. The samples were allowed to equilibrate for 3 min before analysis (mean ± SEM) (n = 5 at each temperature).

TABLE 3. The osmotically inactive cell fraction, V_b, of human sperm obtained using an electronic particle counter and the BVH relationship.

Temperature (°C)	V_b (%)	Sample size (n)	CV[a] among donors (%)
22	50.0 ± 1.0[b]	5	5.4
11	41.0 ± 2.0	5	13.1
0	52.0 ± 3.0	5	12.7
Mean ± SEM across temperature	47.7 ± 3.4		

[a] Coefficient of variation.
[b] Mean ± SEM.

was independent of donor ($p = 0.74$), but dependent upon temperature ($p = 0.03$). The CV among donors was less than 13.1% across each experimental temperature. The average volume (V_b%) across temperature was 48% (Table 3).

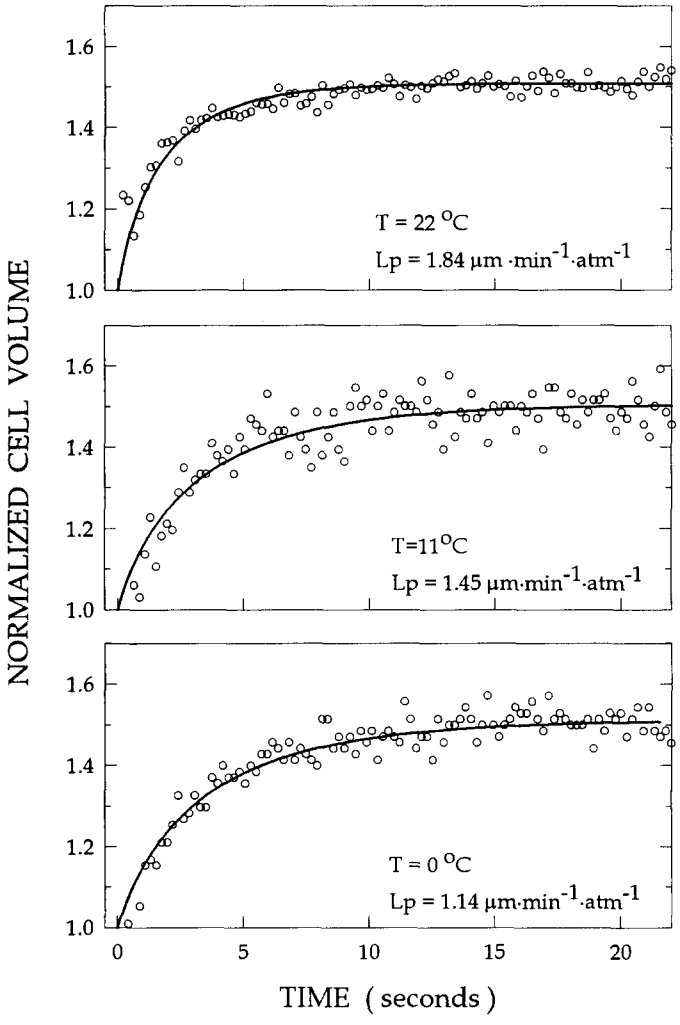

FIG. 3. Representative kinetic volume changes during hyposmotic swelling of human sperm at 22, 11, and 0°C. The isosmotic sperm sample was abruptly diluted into 145 mOsm/kg medium, and the average cell volume was measured over time. A theoretical curve was fit to the experimental data to determine the L_p values (n = 5 at each temperature). Hydraulic conductivities are mean values across donors.

TABLE 4. Hydraulic conductivity of human sperm at different temperatures.

Temperature[a] (°C)	L_p ($\mu m \cdot min^{-1} \cdot atm^{-1}$)	Sample size (n)	CV[b] within donors (%)	CV among donors (%)
22	1.84 ± 0.06[c]	5	20.3	16.9
11	1.45 ± 0.04	5	9.4	12.6
0	1.14 ± 0.07	5	20.3	31.2

[a] There was a significant effect of temperature on L_p ($p = 0.0001$).
[b] Coefficient of variation.
[c] Mean ± SEM.

Experiment 3: Determination of L_p and its E_a in the Absence of CPA

Data from the kinetic volume changes in hyposmotic solutions (Fig. 3) were fitted to equation [6] to compute L_p at 22, 11, and 0°C. The hydraulic conductivity decreased from 1.84 to 1.14 $\mu m \cdot min^{-1} \cdot atm^{-1}$ over the temperature range of 22–0°C (Table 4), yielding an Arrhenius activation energy of 3.48 kcal/mol (Fig. 4). There was no significant main effect of donor on L_p ($p > 0.10$), and the CV among donors was less than 31.2% across each experimental temperature.

CFDA staining was used to monitor membrane integrity during the L_p swelling experiments. Control cells were > 95% CFDA-positive; the percentage of cells exposed to the 145 mOsm/kg solution for 3 min that were CFDA-positive was not different ($p = 0.36$) from the percentage for controls.

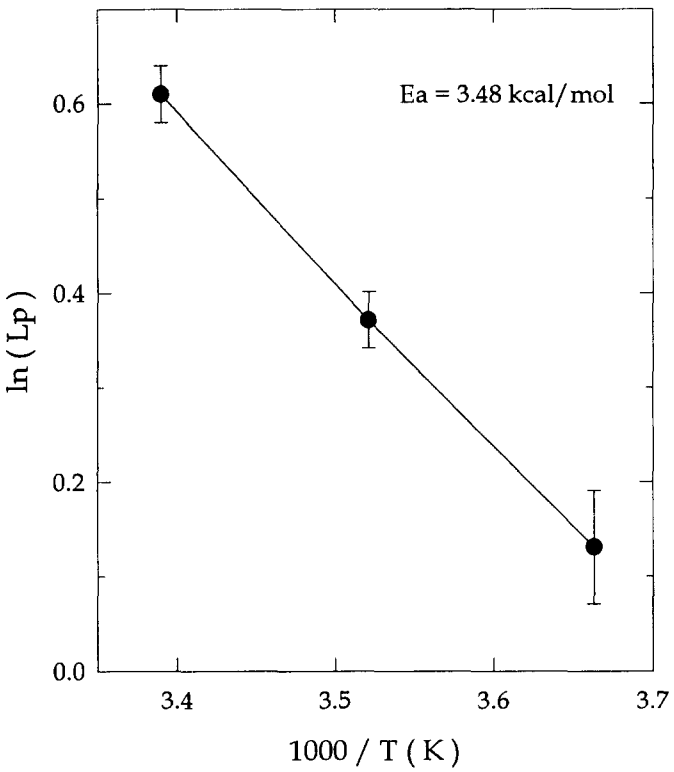

FIG. 4. An Arrhenius plot of the L_p of human sperm: the water permeability was determined at 22, 11, and 0°C (n = 5 at each temperature).

Experiment 4: Determination of P_{CPA} and L_p^{CPA} for Gly, DMSO, PG, and EG

When cells equilibrated with a CPA are abruptly exposed to a solution without CPA, there is a transient increase in cell volume (Fig. 5). These volume data were fitted in order to compute values for L_p^{CPA} (L_p in the presence of CPA) and P_{CPA}. The sperm membrane permeability parameters at 22°C in the presence of the cryoprotectants Gly, DMSO, PG, and EG are shown in Table 5. In the presence of CPAs, the hydraulic conductivity was reduced by an average of 51%. There was no significant main effect of donor on L_p in the presence of CPAs ($p = 0.61$), with the exception of DMSO ($p = 0.003$). Solute permeabilities (P_{CPA}) ranged from a low of 0.80×10^{-3} cm/min (DMSO) to a high of 7.9×10^{-3} cm/min (EG); there was no significant main effect of donor on P_{CPA} ($p = 0.13$) except in the case of EG ($p = 0.0007$). All CVs were less than 31% within and among donors. The reflection coefficient σ (computed from the L_p^{CPA} and P_{CPA} values using the assumption of solute-solvent noninteraction) ranged from 0.77 to 0.98 for EG and DMSO, respectively.

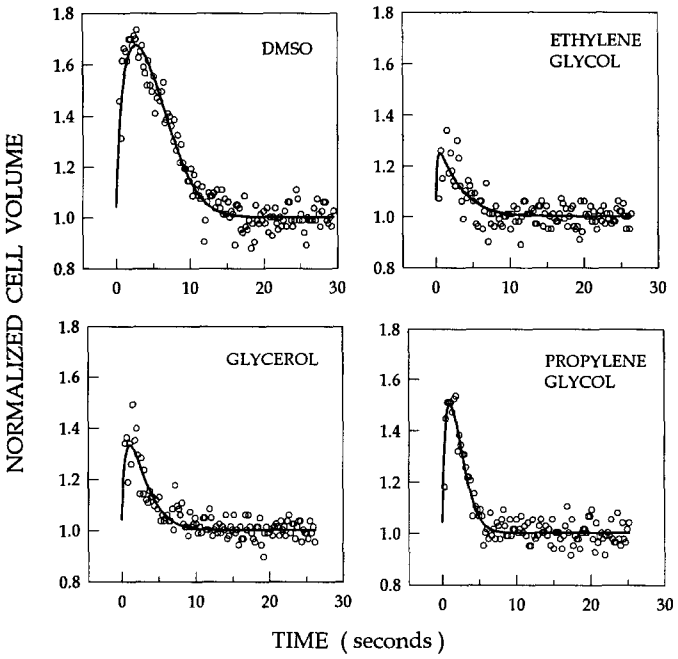

FIG. 5. Kinetic volume changes of human sperm upon dilution of permeant solutes. The initial concentrations were 1) 1 M DMSO, 2) 2 M EG, 3) 1 M Gly, and 4) 1 M PG. Each sample was exposed to the CPA and allowed to equilibrate at room temperature. The sample was then abruptly diluted in an isosmotic solution without CPA and the volume was measured over time. Theoretical curves were fit to the experimental data to determine P_{CPA} and L_p^{CPA}.

DISCUSSION

Isosmotic Cell Volume

Kleinhans et al. [20] have recently reviewed the literature regarding human sperm volume estimates. Recent electronic counter measurements [21, 22] as well as microscopic measurements [23] suggest a human sperm volume in the range of 15–18 μm^3 (although older electronic counter measurements in the literature suggest much larger values, as high as 50–70 μm^3). Other methods such as "volume exclusion" [24] and electron paramagnetic resonance (EPR) [20] suggest a volume in the range 34–37 μm^3. In the present study, the average volume for human sperm across the three experimental temperatures of 22, 11, and 0°C was 28.5 ± 0.3 μm^3, well within the range of recent estimates.

Cell Osmotic Response

Human sperm have previously been shown to exhibit linear osmometric behavior over the range of 250–1500 mOsm/kg [25]. In the present study the observation of a linear response was extended to 145 mOsm/kg at temperatures between 22 and 0°C, which means that the cell volume changes linearly down to 0°C as the reciprocal of external osmolality. From this, one can determine the osmotically inactive fraction of the cell (extrapolation to the Y intercept). This linear behavior and the osmotically inactive fraction are needed to determine the amount of intracellular and extracellular solvent and solute flux, and thus influence the degree to which cells will shrink and swell during freezing. The rate of volume excursion that cells experience during exposure to and removal from anisosmotic solutions is directly related to the rate at which human sperm are cooled and warmed during the cryopreservation process.

Estimation of human spermatozoa cell solids content. It has heretofore been difficult to determine the cell solids content (V_s) of human sperm. Using data available in the literature, Kleinhans et al. [20] estimated V_s as 41% of the total cell volume. Through use of the V_b data from this cur-

TABLE 5. Comparison of human sperm membrane permeabilities at 22° C to CPAs and to water in the presence of CPAs, as well as the associated σ values.

CPA	Concentration (molar)	P_{CPA} (10^{-2} cm/min)	$P_f^{CPA\dagger}$ (10^{-2} cm/min)	L_p^{CPA} ($\mu m \cdot min^{-1} \cdot atm^{-1}$)	σ
Glycerol	1M	0.21 ± 0.01[a]	104 ± 11	0.77 ± 0.08	0.93 ± 0.007
Propylene glycol	1M	0.23 ± 0.01	166 ± 12	1.23 ± 0.09	0.95 ± 0.005
DMSO	1M	0.080 ± 0.002	112 ± 9	0.84 ± 0.07	0.98 ± 0.002
Ethylene glycol	2M	0.79 ± 0.07	100 ± 8	0.74 ± 0.06	0.77 ± 0.044

†L_P^{CPA} expressed as a velocity, $P_f^{CPA} = RTL_p^{CPA}/\overline{V}_w$.
[a] Mean = SEM.

TABLE 6. Examples of cells with water channel-forming proteins.

Cell type	Protein	Hg Inhibition?	L_p ($\mu m \cdot min^{-1} \cdot atm^{-1}$)	Temperature (°C)	E_a (kcal/mol)
Human RBC[a]	CHIP28[b]	Yes	8.9	22	4.0
Renal CCT[c]	WCH-CD[d]	Yes	3.9–39	—	2.0–5.0
Renal PCT[e]	CHIP28[f]	Yes	2.1	22	2.5
Human sperm[g]	(not CHIP28)[h]	No	1.84	22	3.48
Vacuolar membrane	γ-TIP[i]	Yes	—	—	—
Rat lung	MIWC[j]	No	—	—	—

[a] L_p interpolated from 25° C, Moura et al. [40]; E_a from Macey [27].
[b] Preston et al. [29].
[c] Renal cortical collecting tubules; L_p and E_a from Harris Jr. et al. [51].
[d] Fushimi et al. [52].
[e] Renal proximal convoluted tubules; L_p and E_a from Meyer and Verkman [53].
[f] Denker et al. [54].
[g] This work.
[h] Liu et al. [28].
[i] Maurel et al. [55].
[j] Hasegawa et al. [30].

rent work and the previously reported EPR data of Du et al. [25], an independent estimate of V_s is now possible. The EPR spin label method measures the total water content of the cells (V_w), and an EPR BVH plot y-intercept yields the osmotically inactive water (V_a) in the cell. The current data indicate that the human sperm V_b value is 50% at room temperature, and Du et al. [25] report a Ponder's $\boldsymbol{R}$ value of 0.867. Expressed in terms of Ponder's $\boldsymbol{R}$, V_a is given by:

$$V_a = (1-\boldsymbol{R})V_w. \quad [8]$$

The Coulter counter measures total cell volume (V), which is the sum of the cell water (V_w) and the cell solids (V_s),

$$V = V_w + V_s, \quad [9]$$

and a Coulter counter BVH plot intercept yields the osmotically inactive cell volume (V_b), which includes both the cell solids (V_s) and the osmotically inactive water (V_a):

$$V_b = V_s + V_a. \quad [10]$$

Combining equations [8], [9], and [10] yields:

$$V_s\,(\%) = \frac{V_b - (1 - \boldsymbol{R})\,V}{\boldsymbol{R}}. \quad [11]$$

If V_s and V_b are expressed as a percentage of the total cell volume (V), equation [11] becomes:

$$V_s\,(\%) = \frac{V_b\,(\%) - 100\%\,(1 - \boldsymbol{R})}{\boldsymbol{R}}. \quad [12]$$

For completeness, we note that the total cell water (V_w) is simply the sum of the osmotic water (V_{ow}) and the osmotically inactive water (V_a):

$$V_w = V_{ow} + V_a. \quad [13]$$

Using equation [12], the data from Du et al. [25], and the data from this current work, it is then possible to solve for the human sperm cell V_s, which yields a value of 42% solids—very close to the previous estimate of 41% obtained by independent means. The other volume percentages are V_b = 50% (experimentally measured osmotically inactive cell volume) and V_a = 8% (osmotically inactive water from equation [10]).

Water Permeability and Activation Energy Without CPA

The hydraulic conductivity of human sperm was previously measured by Noiles et al. [3] using a "time-to-lysis" method and found to be 2.4 $\mu m \cdot min^{-1} \cdot atm^{-1}$. Recalculating this value using the cell volume reported in their study yields an L_p of 2.1 $\mu m \cdot min^{-1} \cdot min^{-1}$, comparable to the L_p reported in the present study. The similar results obtained with different techniques ("time-to-lysis" and Coulter counter) support the use of the Coulter counter with its advantages of greater time resolution and accuracy.

The two methods also yield similar activation energies. Noiles et al. [3] report an E_a of 3.93 kcal/mol over the temperature range 30° to −7°C, and the electronic counter data yield an E_a of 3.48 kcal/mol over the temperature range 22 to 0°C.

A comparison of L_p for human sperm with that of sperm of other species has been previously presented by Noiles et al. [3]. Human sperm and those of some other species (fowl and cattle [26]) have a high L_p and low E_a; this is considered indicative of water channels [27]. Human sperm may belong to a small group of cell types whose plasma membranes contain channel-forming proteins selective for water [28], with a high L_p and low E_a (Table 6). Human RBC, the best characterized of these cells, utilize the CHIP28 channel protein [29], which is sensitive to inhibition by mercurial compounds. Mercurial inhibition of water transporters has generally been considered a common characteristic of such proteins. However, the recent discovery of mercurial insensitivity in human sperm [28] indicates that the high water permeability may be a result of a unique lipid membrane

structure or of the existence of other types of water channels. The existence of such a mercurial-insensitive water channel has recently been reported in rat lung tissue [30].

Permeability of Cells to Cryoprotectants

Gly has been the conventional CPA for cryopreservation of spermatozoa [31]. However, osmotic damage and subsequent cell injury or death resulting from current standard methods of human sperm cryopreservation incorporating the use of Gly is still very high (~ 50%). Therefore, other permeating solutes need to be investigated [4]. By determining the permeability of human sperm cells to various cryoprotectants, mathematical modeling can be used to ascertain the most appropriate method for adding the CPA before freezing and for removing the CPA after freezing and thawing.

Of the solutes tested, DMSO had the lowest permeability in human sperm cells (0.80×10^{-3} cm/min), while Gly and PG permeated at similar rates (2.1×10^{-3} cm/min and 2.3×10^{-3} cm/min, respectively). The permeability values obtained from this approach for Gly are similar to values derived from other approaches [4] and also fit well within the range for room temperature permeability coefficients of other cell types. Du et al. [6] discuss in detail the permeability of various cell types to Gly. Specifically, the range for the permeability of human sperm to Gly was found to be 8.2×10^{-4} to 1.5×10^{-3} cm/min ([6] and [5], respectively). The permeability of DMSO has been measured in human granulocytes [32], cultured megakaryocytopoietic cells of the rat [33], and human platelets [34] and found to be 2.1×10^{-3}, 9.3×10^{-4}, and 7.8×10^{-4} cm/min, respectively. EG permeability has been measured in human platelets [35] and RBC [36] and found to be 1.0×10^{-3} and 8.9×10^{-3} cm/min, respectively. The rate of PG permeation has been measured in human platelets [37] and RBC [38] and found to be 1.7×10^{-3} and 1.9×10^{-3} cm/min, respectively. Although solute permeability rates may be similar among some cell types, it is important to recognize that P_{CPA} depends on the structure and composition of the membrane and that therefore rates are likely to be different among cell types and within a cell type among species.

In the present study, EG had the highest permeability of the solutes tested (7.94×10^{-3} cm/min). This rate is about ten times that for DMSO and more than three times greater than for Gly and PG. Other studies have shown a high permeability of EG in mouse zygotes and embryos [39]. This finding suggests that EG may be a more optimal solute for cryopreservation, causing minimal cell volume excursion during freezing and thawing due to the high rate of permeation, depending on the activation energy of P_{EG}. It may be that fewer steps will be required for addition and removal of EG as opposed to Gly (which requires a multistep process [4]), potentially making EG a more optimal solute for cryopreservation.

Reflection Coefficient, Sigma

Frequently the presumption is made that the Kedem-Katchalsky [13] transport model requires that σ be close to 1 if the solute and solvent (water) cross the membrane via independent pathways. The correct statement [13] is: $\sigma \leq 1 - P_{CPA}\overline{V}_{CPA}/P\overline{V}_w = 1 - P_{CPA}/(RTL_p^{CPA})$, where the equals sign holds for the case of independent fluxes and $\overline{V}_{CPA}$ and $\overline{V}\,N_w$ are the partial molal volumes of cryoprotectant and water, respectively, and P_f is simply L_p^{CPA} expressed dimensionally as a velocity ($P_f = RTL_p^{CPA}/\overline{V}_w$). Within the Kedem-Katchalsky formalism, a solute-solvent interaction implies that the solute and solvent are using (at least in part) the same "channel" for transport and consequently that there is a physical interaction of the two fluxes with each other. Diffusion of the solute and solvent across the bilayer is a noninteracting transport process and the above equality for σ holds. This does not necessarily imply that the solute will not modify the membrane in a fashion that affects the transport of water.

In the current experiments, the value of σ was fixed at its noninteracting value for two reasons. First, a growing body of evidence [27, 29] suggests (at least for the well-studied case of human RBC) that in cells with a high L_p and low E_a, water transport occurs primarily through highly selective ("primary") water channels and that transport of nonionic solutes occurs through the bilayer or through channels that are distinct from the primary water channels. Second, σ is poorly constrained by our experimental data. This is typical in experiments of this nature in which cell response is primarily determined by the values of L_p and P_{CPA} and to a lesser extent by σ. Thus, it seemed prudent to fix σ at its noninteracting value. This was done by replacing σ by the expression $(1 - P_{CPA}\overline{V}_{CPA}/(RTL_p^{CPA})$ in equations [8] and [9]. This is equivalent to characterizing the membrane by a two-parameter (L_p and P_{CPA}) transport model as described in Du et al. [6].

Interestingly, for the case of EG transport in human sperm, imposition of noninteraction on σ yields a value of $\sigma = 0.77$ because of a high P_{CPA} and low L_p^{CPA} value (Table 5). This is an explicit example of a situation in which noninteraction of the solute and solvent can yield a σ significantly less than 1, and it is the lowest noninteracting value of σ we are aware of for a nonionic solute crossing a cell membrane or artificial lipid bilayer.

Water Permeability in the Presence of CPA

The addition of a cryoprotectant to a sperm suspension was hypothesized to affect (lower) the hydraulic conductivity. Studies of human RBC [27, 40] have shown that approximately 90% of the RBC membrane water flux is carried by protein channels and that 10% passes through the lipid bilayer. Given these two routes of water movement, a nonionic solute could affect the membrane permeability in at least three ways. First,

the solute could modify the bilayer, causing a change in bilayer permeability [41]. Second, a modification of the bilayer could indirectly affect membrane transporter protein activity [42]. Third, the solute could interfere directly with the function of the water-transporting proteins (either primary water channels specific for water transport like CHIP 28, or secondary water channels that are presumably for some other molecule, like glucose, but that also facilitate water transport). This last possibility seems to be the case in the human RBC investigations of Toon and Solomon [43, 44].

If some period of incubation is required for solute modification of the membrane permeability to water, then we can expect the timing of the cell exposure to solute to be of importance. The easiest experiments to interpret are those in which cells are preexposed to a solute and remain in the solute during the course of the experiment. Such experiments have been done with human RBC and show a significant CPA concentration-dependent inhibition of water transport by Gly [45] and EG [44, 45]. Similar results have been reported for lung fibroblasts exposed to DMSO or Gly [46].

In addition, Toon and Solomon [43] and van Hoek et al. [47] have shown that the inhibitory effect of urea on human RBC L_p and DMSO on rat kidney brush border membrane vesicle L_p is reversible by washing the cells/vesicles free of solute. Their data do not address the question of the time required for solute inhibition of L_p or reversal by washing.

In the experiments reported here, the cells were preexposed to the CPA solute that is "washed out" beginning at time zero of the L_p^{CPA} determination. The timing is such that the solute concentration is calculated to be reduced to less than 10% of its initial concentration in 3 sec, while the L_p measurement takes 5–10 sec to execute (Fig. 5).

Other investigators have also found solute inhibition of L_p in similarly designed experiments [33, 48]. Thus, either L_p^{CPA} is changing during the course of these experiments as the solute concentration drops and the measured L_p^{CPA} is an average value or the inhibitory effect of the solute is not rapidly reversible and L_p^{CPA} remains constant during the course of the experiment. Further work will be required to resolve this question.

In the current experiments with human sperm, PG, DMSO, Gly, and EG were found to reduce L_p by 33% to 60% at 22°C, yielding L_p^{CPA} values of 1.23, 0.84, 0.77 and 0.74 $\mu m \cdot min^{-1} \cdot atm^{-1}$, respectively. One hypothesis to explain these results is that these CPAs are blocking (directly or via bilayer modification) either primary or secondary water channels in the human sperm membrane and thereby reducing L_p to its "background" bilayer value. Moura et al. [40] reported a background bilayer L_p for human RBC of 0.65 $\mu m \cdot min^{-1} \cdot atm^{-1}$ (extrapolated from 25°C to 22°C using an E_a of 12 kcal/mol; Fettiplace and Haydon [49]), which is comparable to the above L_p^{CPA} values of human sperm in the presence of DMSO, Gly, and EG.

If this hypothesis is correct, then the human sperm membrane should have the following characteristics: 1) in the absence of water channel blocking (directly or indirectly), the human sperm membrane should have a high L_p and low E_a; 2) in the presence of channel blocking, L_p should decrease to a value typical of bilayer-only transport (diffusion); and 3) the activation energy for water transport should approach the high values found for lipid bilayer membranes. The first point has been established by Noiles et al. [3] and by the present study. As to the second point, the present work demonstrates a reduction of human sperm L_p in the presence of DMSO, Gly, or EG to a value comparable to that found for human RBC bilayer transport; this is consistent with the hypothesis that these CPAs are interfering with the function of a putative primary or secondary water channel. We are currently investigating the third point, and preliminary experiments suggest that the E_a of L_p does increase in the presence of CPAs.

Although the mechanism of the CPA reduction of human sperm plasma membrane water permeability is unresolved, these experiments indicate a marked effect of CPAs on water permeability. They also demonstrate the utility of an electronic particle counter for the determination of sperm membrane permeability characteristics. The knowledge from this study is important for efforts to optimize the cryopreservation of human spermatozoa. Cooling and warming rates are determined on the basis of these permeability properties. A reduction in hydraulic conductivity would require a reduction in cooling rate. Theoretical studies using L_p in the absence of CPA have shown that human sperm should tolerate high cooling rates and still allow for sufficient time for water to diffuse extracellularly and prevent intracellular ice formation [3]. However, attempts to empirically confirm these cooling rates (800°C/min) have resulted in cell death [8, 50]. It has been hypothesized that L_p may be influenced by the presence of CPAs [3]; however, to date it has been difficult to measure water permeability in the presence of cryoprotectants. The current study has developed a method of resolving this issue and has shown that there is a decrease in L_p in the presence of CPAs. Our observed decrease in L_p at 22°C is insufficient to explain the predicted optimal cooling rate discrepancies between theory and practice. However, preliminary work shows that the E_a of L_p^{CPA} is much higher than the E_a of L_p. Thus the extrapolated value of L_p^{CPA} to sub-zero temperatures may be substantially reduced, and this would explain, at least in significant part, this current discrepancy between theory and practice.

Additionally, optimal cryoprotectant solutes, and the most effective means for their addition and removal, can be determined from knowledge of these permeability properties. Collectively, these data provide a foundation for similar investigations to be performed with the sperm of other species that historically have been more difficult to study and that have lower spermatozoa cryosurvival than the human, such as the mouse and the boar.

ACKNOWLEDGMENTS

The authors would like to thank Dr. Paul Watson (Royal Veterinary College, University of London) and Dr. Peter Mazur (Oak Ridge National Laboratory, Oak Ridge, TN) for helpful discussion of the manuscript and Katherine Vernon for manuscript preparation.

REFERENCES

1. Mascola L, Guinan ME. Screening to reduce transmission of sexually transmitted disease in semen used for artificial insemination. N Engl J Med 1986; 314:1354–1359.
2. Mazur P. Freezing of living cells: mechanisms and implications. Am J Physiol 1984; 247:C125-C142.
3. Noiles EE, Mazur P, Watson PF, Kleinhans FW, Critser JK. Determination of water permeability coefficient for human spermatozoa and its activation energy. Biol Reprod 1993; 48:99–109.
4. Gao DY, Liu J, Liu C, McGann LE, Watson PF, Kleinhans FW, Mazur P, Critser ES, Critser JK. Prevention of osmotic injury to human spermatozoa during addition and removal of glycerol. Hum Reprod 1995; 10:1109–1122.
5. Gao DY, Mazur P, Kleinhans FW, Watson PF, Noiles EE, Critser JK. Glycerol permeability of human spermatozoa and its activation energy. Cryobiology 1992; 29:657–667.
6. Du Junying, Kleinhans FW, Mazur P, Critser JK. Human spermatozoa glycerol permeability and activation energy determined by electron paramagnetic resonance. Biochim Biophys Acta 1994; 1194:1–11.
7. Sherman JK. Dimethyl sulfoxide as a protective agent during freezing and thawing of human spermatozoa. Proc Soc Exp Biol Med 1964; 117:261–264.
8. Henry MA, Noiles EE, Gao DY, Mazur P, Critser JK. Cryopreservation of human spermatozoa. IV: The effects of cooling rate and warming rate on the maintenance of motility, plasma membrane integrity, and mitochondrial function. Fertil Steril 1993; 60:911–918.
9. McGann LE, Turner AR, Turc JM. Microcomputer interface for rapid measurements of cell volume using an electronic particle counter. Med Biol Eng & Comput 1982; 20:117–120.
10. Brotherton J. Calibration of the counter model A for the size determination of the cell. Proc Soc Anal Chem 1971; 264–271.
11. Bavister BD, Leibfried ML, Lieberman G. Development of preimplantation embryos of the golden hamster in a defined culture medium. Biol Reprod 1983; 28:235–247.
12. Gao DY, Ashworth E, Watson PF, Kleinhans FW, Mazur P, Critser JK. Hyperosmotic tolerance of human spermatozoa: separate effects of glycerol, sodium chloride, and sucrose on spermolysis. Biol Reprod 1993; 49:112–123.
13. Kedem O, Katchalsky A. Thermodynamic analysis of the permeability of biological membranes to nonelectrolytes. Biochim Biophys Acta 1958; 27:229–246.
14. Weast RC. Handbook of Chemistry and Physics. 51st Ed. Cleveland, OH: The Chemical Rubber Co.; 1970–1971.
15. Kiyohara O, Perron G, Desnoyers JE. Volumes and heat capacities of dimethylsulfoxide, acetone, and acetamide in water and of some electrolysis in these mixed aqueous solvents. Can J Chem 1975; 52:3263–3268.
16. Dick DAT. Cell Water. Washington: Butterworths; 1966.
17. Press WH, Flannery BP, Teukolsky SA, Vetterling WT. Numerical Recipes: The Art of Scientific Computing. Cambridge: Cambridge University Press; 1986.
18. Levin RL, Cravalho EG, Huggins CE. A membrane model describing the effect of temperature on water conductivity of erythrocyte membranes at subzero temperatures. Cryobiology 1976; 13:419–429.
19. Gao DY, Liu C, Benson C, Liu J, McGann LE, Lin S, Critser ES, Crister JK. Theoretical and experimental analyses of optimal experimental design for determination of hydraulic conductivity of cell membrane. In: Hayes LJ, Roemer RB (eds.), Advances in Heat and Mass Transfer in Biological Systems, HTD-Vol. 228. New York: ASME Press; 1994: 151–158.
20. Kleinhans FW, Travis VS, Du Junying, Villines PM, Colvin KE, Critser JK. Measurement of human sperm intracellular water volume by electron spin resonance. J Androl 1992; 13:498–506.
21. Laufer N, Segal S, Yaffe H, Svartz H, Gover NB. Volume and shape of normal human spermatozoa. Fertil Steril 1977; 28:456–458.
22. Jeyendran RS, Karuhn RF, Van Der Ven HH, Perez-Pelaez M. Volumetric analysis of human spermatozoa. Andrologia 1987; 19:54–57.
23. Van Duijn C Jr. II. Biometry of human spermatozoa. J Roy Microsc Soc 1957; 77:12–27.
24. Ford WCL, Harrison A. D-[1–14C] mannitol and [U-14C] sucrose as extracellular space markers for human spermatozoa and the uptake of 2-deoxyglucose. J Reprod Fertil 1983; 69:479–487.
25. Du Junying, Kleinhans FW, Mazur P, Critser JK. Osmotic behavior of human spermatozoa studies by EPR. Cryo Lett 1993; 14:285–294.
26. Watson PF, Kunze E, Cramer P, Hammerstedt RH. A comparison of critical osmolality, hydraulic conductivity and its activation energy in fowl and bull spermatozoa. J Androl 1992; 13:131–138.
27. Macey RI. Transport of water and urea in red blood cells. Am J Physiol 1984; 246(Cell Physiol 15):C195-C203.
28. Liu C, Gao DY, Preston GM, McGann LE, Benson CT, Critser ES, Critser JK. The high water permeability of human spermatozoa is mercury resistant and not mediated by CHIP28. Biol Reprod 1995; 52:913–919.
29. Preston GM, Carroll TP, Guggion WB, Agre P. Appearance of water channels in *Xenopus* oocytes expressing red cell CHIP28 protein. Science 1992; 256:385–387.
30. Hasegawa H, Ma T, Skach W, Matthay MA, Verkman AS. Molecular cloning of mercurial-insensitive water channel expressed in selected water-transporting tissues. J Biol Chem 1994; 269:5497–5500.
31. Sherman JK. Synopsis of the use of frozen human semen since 1964: state of the art of human semen banking. Fertil Steril 1973; 24:397–416.
32. Toupin CJ, Le Maguer M, McGann LE. Permeability of human granulocytes to dimethyl sulfoxide. Cryobiology 1989; 26:422–430.
33. Hempling HG, White S. Permeability of cultured megakaryocytopoitic cells of the rat to dimethyl sulfoxide. Cryobiology 1984; 21:133–143.
34. Law P, Hempling HG, Burton JL, Douglas M. Permeability of human platelets to dimethylsulfoxide and glycerol. Cryobiology 1986; 23:555 (abstract).
35. Meyer MM, Verkman AS. Human platelet osmotic water and nonelectrolyte transport. Am J Physiol 1986; 251:C549-C557.
36. Savitz D, Solomon AK. Tracer determinations of human red cell membrane permeability to small nonelectrolytes. J Gen Physiol 1971; 58:259–266.
37. Arnaud FG, Pegg DE. Permeation of glycerol and propane-1,2-diol into human platelets. Cryobiology 1990; 27:107–118.
38. Macey RI, Karan DM. Independence of water and solute pathways in human RBCs. J Membr Biol 1993; 134:241–250.
39. Leibo SP, Oda K. High survival of mouse zygotes and embryos cooled rapidly or slowly in ethylene glycol plus polyvinylpyrrolidone. Cryo Lett 1993; 14:133–144.
40. Moura TF, Macey RI, Chien DY, Karan D, Santos H. Thermodynamics of all-or-none water channel closure in red cells. J Membr Biol 1984; 81:105–111.
41. Hammerstedt RH, Graham JK, Nolan JP. Cryopreservation of mammalian sperm: what we ask them to survive. J Androl 1990; 11:73–88.
42. Carruthers A, Melchior DL. How bilayer lipids affect membrane activity. TIBS 1986; 11:331–335.
43. Toon MR, Solomon AK. Modulation of water transport in human red cells: effects of urea. Biochim Biophys Acta 1988; 940:266–274.
44. Toon MR, Solomon AK. Transport parameters in the human red cell membrane: solute-membrane interactions of hydrophilic alcohols and their effect on permeation. Biochim Biophys Acta 1990; 1022:57–71.
45. Papanek TH. The water permeability of the human erythrocyte in the temperature range +25°C to −10°C. MIT; 1978. Ph.D. Thesis.
46. Rule GS, Law P, Kruuv J, Lepock JR. Water permeability of mammalian cells as a function of temperature in the presence of dimethylsulfoxide: correlation with the state of the membrane lipids. J Cell Physiol 1980; 103:407–416.
47. van Hoek AN, de Jong MD, van Os CH. Effects of dimethylsulfoxide and mercurial sulfhydryl reagents on water and solute permeability of rat kidney brush border membranes. Biochim Biophys Acta 1990; 1030:203–210.
48. Connolly A, Hempling HG. The effects of dimethyl sulfoxide on the osmotic properties of a rat megakaryocytopoietic cell line. Cryobiology 1985; 22:351–358.
49. Fettiplace R, Haydon DA. Water permeability of lipid membranes. Physiol Rev 1980; 60:5510–5550.
50. Curry MR, Millar JD, Watson PF. Calculated optimal cooling rates for ram and human sperm cryopreservation fail to conform with empirical observations. Biol Reprod 1994; 51:1014–1021.
51. Harris HW Jr, Strange K, Zeidel ML. Current understanding of the cellular biology and molecular structure of the antidiuretic hormone-stimulated water transport pathway. J Clin Invest 1991; 88:1–8.
52. Fushimi K, Uchida S, Hara Y, Hirata Y, Marumo F, Sasaki S. Cloning and expression of apical membrane water channel of rat kidney collecting tubule. Nature 1993; 361:549–552.
53. Meyer MM, Verkman AS. Evidence for water channels in renal proximal tubule cell membranes. J Membr Biol 1987; 96:107–119.
54. Denker BM, Smith BL, Kuhajda FP, Agre P. Identification, purification, and partial characterization of novel M_r 28 000 integral membrane protein from erythrocytes and renal tubules. J Biol Chem 1988; 263:15634–15642.
55. Maurel C, Reizer J, Schroeder JI, Chrispeels MJ. The vascular membrane protein τ-TIP creates water specific channels in *Xenopus* oocytes. EMBO J 1993; 12:2241–2247.